Use of Carbon Oxysulfide, a Structural Analog of CO₂, to Study Active CO₂ Transport in the Cyanobacterium *Synechococcus* UTEX 625[1]

Anthony G. Miller*, George S. Espie[2], and David T. Canvin

Department of Biology, Queen's University, Kingston, Ontario, Canada, K7L 3N6

ABSTRACT

Carbon oxysulfide (carbonyl sulfide, COS) is a close structural analog of CO_2. Although hydrolysis of COS (to CO_2 and H_2S) does occur at alkaline pH (>9), at pH 8.0 the rate of hydrolysis is slow enough to allow investigation of COS as a possible substrate and inhibitor of the active CO_2 transport system of *Synechococcus* UTEX 625. A light-dependent uptake of COS was observed that was inhibited by CO_2 and the ATPase inhibitor diethylstilbestrol. The COS taken up by the cells could not be recovered when the lights were turned off or when acid was added. It was concluded that most of the COS taken up was hydrolyzed by intracellular carbonic anhydrase. The production of H_2S was observed and COS removal from the medium was inhibited by ethoxyzolamide. Bovine erythrocyte carbonic anhydrase catalysed the stoichiometric hydrolysis of COS to H_2S. The active transport of CO_2 was inhibited by COS in an apparently competitive manner. When Na^+-dependent HCO_3^- transport was allowed in the presence of COS, the extracellular $[CO_2]$ rose considerably above the equilibrium level. This CO_2 appearing in the medium was derived from the dehydration of transported HCO_3^- and was leaked from the cells. In the presence of COS the return to the cells of this leaked CO_2 was inhibited. These results showed that the Na^+-dependent HCO_3^- transport was not inhibited by COS, whereas active CO_2 transport was inhibited. When COS was removed by gassing with N_2, a normal pattern of CO_2 uptake was observed. The silicone fluid centrifugation method showed that COS (100 micromolar) had little effect upon the initial rate of HCO_3^- transport or CO_2 fixation. The steady state rate of CO_2 fixation was, however, inhibited about 50% in the presence of COS. This inhibition can be at least partially explained by the significant leakage of CO_2 from the cells that occurred when CO_2 uptake was inhibited by COS. Neither CS_2 nor N_2O acted like COS. It is concluded that COS is an effective and selective inhibitor of active CO_2 transport.

Cyanobacteria can photosynthesize and grow at very low DIC[3] concentrations because they possess active transport systems for both HCO_3^- and CO_2 (2-4, 7, 8, 12, 18, 22, 23,

[2] Present address: Department of Biology, Concordia University, Montreal, Quebec, Canada H3G 1M8.

[3] Abbreviations: DIC, dissolved inorganic carbon (CO_2 + HCO_3^- + CO_3^{2-}); BTP, 1,3-bis (tris [hydroxymethyl] methylamino)-propane; CA, carbonic anhydrase; COS, carbon oxysulfide (carbonyl sulfide); DES, diethylstilbestrol; EZA, ethoxyzolamide; Rubisco, ribulose bisphosphate carboxylase/oxygenase.

27, 31) that raise the intracellular CO_2 concentration far above that in the extracellular medium and allow the cyanobacterial Rubisco to function in spite of a K_m (CO_2) on the order of 200 μM (1). The whole cell $K_{1/2}$ (CO_2) for photosynthesis of *Synechococcus* UTEX 625 grown in DIC-limited chemostats is 0.008 μM at pH 9.6 (22). CO_2 and HCO_3^- are structurally dissimilar and the mechanisms for active CO_2 and active HCO_3^- transport are probably different (8, 15, 19), and any study on the mechanisms of transport must, of course, make a clear experimental distinction between the two species of inorganic carbon. Active CO_2 transport can be most readily measured by mass spectrometry (2, 3, 19). With the cyanobacterium *Synechococcus* UTEX 625, the contribution of the HCO_3^- transport system can be much reduced or eliminated during measurements of CO_2 transport by simply not providing the cells with the Na^+ needed for HCO_3^- transport (7, 15). Transport of CO_2 in the cyanobacteria proceeds at very low CO_2 concentrations (2, 3, 19) with a $K_{1/2}$ (CO_2) of about 0.4 μM at pH 8.0 (GS Espie, AG Miller, DT Canvin, unpublished data), it requires energy (2, 19), and very high intracellular DIC concentrations can be attained when the rate of supply of CO_2 to the transport system is rapid (3, 15, 19, 31). In some ways CO_2 transport seems to be a more fundamental process than HCO_3^- transport as it is CO_2, not HCO_3^-, that is the DIC species actively transported when *Synechococcus* UTEX 625 is grown on elevated levels of CO_2 (4, 17). In *Synechococcus* UTEX 625, both CO_2 and HCO_3^- transport can occur simultaneously (8) and inhibitor studies (8, 15, 16, 19, 20) suggest that the two transport systems may be separate entities. Our ability to selectively inhibit HCO_3^- transport, by omitting Na^+ from the medium, has been very useful during investigations of the CO_2 transport system (8, 19). The ability to selectively inhibit CO_2 transport would be just as useful. In this paper we report that COS, an isoelectronic structural analog of CO_2, is a selective inhibitor of CO_2 transport by *Synechococcus* UTEX 625. Using this inhibitor we show that a considerable efflux of CO_2 from the cells occurs during HCO_3^- transport. The CO_2 is derived from intracellular dehydration of the actively transported HCO_3^- and can only be seen when the normally efficient CO_2 pump is inhibited.

MATERIALS AND METHODS

Organism and Growth Conditions

Synechococcus UTEX 625 was obtained from the University of Texas (Austin) culture collection. Cells were grown

with air-bubbling as previously described (7) to a Chl concentration of 6 to 8 $\mu g \cdot mL^{-1}$. Cells were then washed and resuspended in 25 mM BTP/HCl buffer at pH 8.0 containing less than 15 μM total DIC (22).

Experimental Conditions

All measurements were performed with 6 mL cell suspensions contained in a thermostated (30°C) glass cuvette that was 20 mm in diameter and that contained a magnetic stirrer bar. The chamber was closed with a tightly fitting Plexiglas plug so as to leave no headspace. The plug contained a capillary bore for injection purposes. The inlet to the MS, sealed into the side of the glass cuvette, was separated from the cell suspension by a thin dimethyl silicone rubber membrane supported by a metal grid. The cell suspensions were placed in the cuvette under N_2 purging to reduce contamination with atmospheric CO_2. The cell density was 6 to 9 μg Chl·mL^{-1}. Illumination was provided by a tungsten-halogen projection lamp. The photon flux density was 220 $\mu E \cdot m^{-2} \cdot s^{-1}$ unless otherwise noted (PAR, measured with a LiCor Model Li 185B light meter).

Measurement of Active CO$_2$ Transport

Changes in the extracellular [CO_2] due to active CO_2 transport were monitored using a membrane inlet system connected to a VG Gas Analysis (model MM-14 80 SC) magnetic sector mass spectrometer, as previously described (8, 19). COS ($m/e = 60$) is partially converted to CS^+ ($m/e = 44$) in the mass spectrometer. A smaller amount (about 1.1%) of $^{13}CS^+$ ($m/e = 45$) is also produced, in accordance with the lower natural abundance of ^{13}C relative to ^{12}C. To avoid large changes in background signal and to be able to identify the source of effluxed CO_2, ^{13}C-DIC was used.

Measurement of Active HCO$_3^-$ Transport

Bicarbonate transport was measured by the silicone fluid centrifugation method (12) essentially as described by Miller and Colman (18). A saturated solution of COS was kept in a serum-stoppered flask and added to the 100 μL samples of cell suspension (at the CO_2 compensation point) as 10 μL aliquots just 15 s before the addition of 10 μL H$^{14}CO_3^-$ solution (25 μM final [DIC], 6.0 $\mu Ci \cdot \mu mol^{-1}$ carbon). Addition of these rather large volumes allows for good mixing of the COS and HCO$_3^-$ with the cell suspension in the microfuge tubes.

Measurement of Photosynthetic CO$_2$ Fixation

In some experiments the illuminated cells in the MS cuvette were provided with H$^{14}CO_3^-$ so that the course of ^{14}C fixation into acid stable products could be followed. A solution containing both H$^{13}CO_3^-$ and H$^{14}CO_3^-$ (2.99 $\mu Ci \cdot \mu mol^{-1}$ carbon) was added to the cell suspension (6 mL) to yield a final [HCO$_3^-$] of 25 μM. Samples of 50 μL were withdrawn at intervals and were injected into 1 mL of methanol. The samples were later analyzed for acid stable ^{14}C activity (7).

Pulse Modulated Fluorimetry

The yield of Chl *a* fluorescence was routinely used to determine when the CO_2 compensation point had been reached and to monitor the progress of DIC transport and CO_2 fixation (16). A pulse amplitude modulation fluorimeter (PAM 101) from Heinz-Walz (Effeltrich, FRG) was used as previously described (20). The degree of quenching obtained upon the initiation of DIC was calculated as previously described (16).

Relevant Physical and Chemical Properties of COS

When pure, COS is an odorless gas but it usually has the odor of rotten eggs due to trace contamination with H_2S. The minimum purity of the COS, available in lecture bottles, from Matheson is 97.5 mol %, with the major contaminants being CS_2 at 0.19%, CO_2 at 1.4%, NO and/or CO at 0.6%, O_2 at 0.10%, and H_2S at 0.01%. The COS from Union Carbide is similar (GH Lorimer, personal communication). At a partial pressure of 1 atm at 13.5°C, COS has a solubility in water of about 34 mM (10). COS is stable when dissolved in acidified water but is hydrolyzed in alkaline solution to CO_2 and H_2S (10, 25, 29). Hydrolysis proceeds via the monothiocarbonate ion which is unstable at low ionic strength at room temperature (25, 29). The rate of COS hydrolysis is slow enough at pH 8.0 or below to allow experiments to be easily performed. The COS molecule, like that of CO_2, is linear and its orbital structure corresponds to that of CO_2 (10). In general, the physical and chemical properties of COS are intermediate between those of CO_2 and CS_2 (10). COS is a toxic gas, presumably because it is broken down to H_2S in the body (5).

Determination of [COS]

Changes in the [COS] in cell suspensions were monitored by mass spectrometry ($m/e = 60$). The COS molecules can cross the membrane of the inlet quite readily, but the overall MS response time for COS measurement was longer than for CO_2 measurement ($t_{0.63}$ of 6 s compared to 2 s). The leak rate of COS into the mass spectrometer was about 0.9%·min^{-1}, measured at pH 6.0 and assuming no loss of COS by hydrolysis. Stock COS solutions were prepared freshly every hour in 0.02 N HCl, by briefly purging the acid with COS from a lecture bottle. The flask was sealed with a gas-tight Suba-seal (Thomas Scientific) and Parafilm. The [COS] in these acidic stock solutions was determined by injecting a 10 μL sample into the MS cuvette containing 6 mL of BTP buffer (25 mM) at pH 10.6. At this pH the COS was rapidly hydrolyzed (see later). After complete hydrolysis of the COS (monitored at $m/e = 60$), the amount of HS$^-$ formed was measured by acidifying the solution with 110 μL 2 N HCl to lower the pH to about 7.0. The resulting [H_2S] (pK$_a$ = 6.9) was monitored at $m/e = 34$. The response at $m/e = 34$ was then calibrated by adding known concentrations of Na$_2$S·9H$_2$O. Since the response at $m/e = 34$ was calibrated internally for each COS determination, the exact pH which was obtained upon addition of the 110 μL 2 N HCl was not critical. The Na$_2$S·9H$_2$O used to prepare the primary standard for the COS determination is a hydroscopic solid capable of being oxidized by air.

The $Na_2S \cdot 9H_2O$ used was nonyellowed and the crystals were quickly washed with distilled water and blotted dry before being weighed. The [HS⁻] in the calibration solutions was determined by spectrophotometry at 230 nm (11). The measured [HS⁻] was within 1% of the nominal concentration. The $Na_2S \cdot 9H_2O$ was dissolved in N_2-purged water to prevent HS⁻ oxidation.

Chemicals

The COS was obtained in lecture bottles from both Matheson (Whitby, Ontario) and Union Carbide (Linde Division, Canbury, CT 06817). Similar results were obtained with the COS from both sources. The CO_2 content could possibly have been reduced by passage of the gas through 30% KOH solution, which unlike more dilute alkali solutions, does not catalyze COS hydrolysis (10). However, scrupulous drying of the gas following its passage through the KOH solution must then be performed if rapid COS hydrolysis is to be prevented (10). Given the possibility of enhanced CO_2 production, the low initial CO_2 contamination of the commercial COS, its toxicity and expense, the COS was used from the lecture bottles without further purification. Control experiments (see later) showed that even if the COS had been completely hydrolyzed to CO_2 and H_2S it would not have given the observed results attributable to COS.

The N_2O was obtained from Canadian Oxygen, Kingston, Ontario. The CS_2 and $Na_2S \cdot 9H_2O$ were from BDH. Bovine erythrocyte CA (2500 WA units·mg⁻¹ protein) and BTP were from Sigma. The $K_2^{13}CO_3$ (99 atom %) was from MSD Isotopes, Montreal.

RESULTS

Stability of COS at pH 8.0

When using COS as a structural analog of CO_2, one must be careful to avoid artifacts due to the hydrolysis of COS to CO_2 and H_2S (10, 25, 29). We have found pH 8.0 to be convenient for the study of HCO_3^- and CO_2 transport by *Synechococcus* UTEX 625 (7, 8, 15–20). At pH 8.0 the $[CO_2]$ at [DIC] ≤ 100 μM is high enough to allow accurate measurement by MS, and the rate of HCO_3^- dehydration is slow enough that active CO_2 transport causes large, easily measurable declines in the $[CO_2]$ (8, 19). Also, at pH 8.0 we know that with air-grown cells 25 mM Na⁺ is required for maximum rates of HCO_3^- transport (7, 15). At pH 8.0 the spontaneous rate of COS hydrolysis is low (Fig. 1A) with a rate constant of 2.2%·min⁻¹ after correction for COS leakage into the MS (0.9% min⁻¹). At more alkaline pH, however, the spontaneous rate of COS hydrolysis becomes significant (Fig. 1A), and at pH 10.6 the rate is rapid enough to allow for the quantitative conversion of COS to HS⁻ in a short time (Fig. 1B).

Carbonic anhydrase not only catalyses the addition of OH⁻ to the carbon-oxygen double bond of CO_2, but also to the double bond in various aldehydes, arylcarboxylate esters, and ammonium carbamate (26). Chengelis and Neal (5) reported that carbonic anhydrase catalyzed the hydrolysis of COS to monothiocarbonate, CO_2 and H_2S. We confirm the finding that CA catalyzes the hydrolysis of COS (Fig. 2). Hydrolysis

was faster at pH 8.0 than pH 6.4 (Fig. 2A), as predicted from the effect of pH on the k_{cat} for the CO_2 hydration reaction (26). Unlike Chengelis and Neal (5), we found no evidence for the accumulation of significant amounts of the unstable monothiocarbonate ion intermediate during the course of the reaction (Fig. 2C). The CA-mediated hydrolysis reaction was carried out at pH 7.0 so that enough H_2S would be present ($pK_a = 6.9$) to be monitored by MS (Fig. 2B). At pH 7.0 there was a 1:1 stoichiometry between COS disappearance and H_2S + HS⁻ production during the entire course of the reaction (Fig. 2C). The addition of acid at any time during the reaction did not cause an increase in the [COS] (data not shown). This result, and the 1:1 stoichiometry between COS breakdown and H_2S + HS⁻ production, demonstrates that the concentration of the monothiocarbonate intermediate remained low. The time course of CO_2 production was complicated by the concomitant decline in the $m/e = 44$ signal due to the disappearance of COS (and thus a reduced rate of CS⁺ formation in the MS) and the increase in $m/e = 44$ signal due to CO_2 production.

COS Uptake by Cells

In the presence of illuminated cells the rate of COS disappearance at pH 8.0 was increased (Fig. 3A). The rate of disappearance of COS in the dark and the presence of cells (Fig. 3A) was similar to that observed in the absence of cells (cf. Fig. 1A). The increased rate of COS disappearance in the light was inhibited by the CO_2 transport and ATPase inhibitor DES (Fig. 3A) and the CA inhibitor EZA (Fig. 3B). At pH 6.95, the addition of cells to a COS solution in the light resulted in the breakdown of COS to H_2S/HS⁻ (Fig. 4). Very little COS breakdown occurred when cells were added in the dark (Fig. 4). There was a close to 1:1 stoichiometry of H_2S/HS⁻ production and COS disappearance (Fig. 4). The accumulation of H_2S/HS⁻ in the medium inhibits COS uptake (see Fig. 3D) and soon reduces the rate of further COS breakdown (Fig. 4). In some experiments, as the rate of COS breakdown decreased (due to an increase in the [H_2S + HS⁻]), there was a decline in the [H_2S + HS⁻] (data not shown). The reason for this decline is not known. It is possible the disappearance of the [H_2S + HS⁻] could have been due to oxidation. The solutions used in these experiments (Fig. 4) were vigorously gassed with N_2 to remove O_2, but the uptake of COS by *Synechococcus* results in O_2 evolution (data not shown). During calibration by the addition of aliquots of $Na_2S \cdot 9H_2O$ solution, a steady decline in the $m/e = 34$ signal was sometimes observed. If the solutions are vigorously purged with N_2 and the H_2S/HS⁻ production is monitored soon after addition of cells, then good stoichiometries are observed (Fig. 4).

The COS that disappeared in the presence of illuminated cells did not reappear when the pH was suddenly lowered below 2.0 or when the cells were darkened (data not shown). This suggests that most of the COS disappearance was due to hydrolysis and not accumulation within the cells. The uptake of COS into the cells in the light, where it would be accessible to hydrolysis by intracellular CA, could be prevented by DES, DIC, or Na_2S (Fig. 3, A, C, and D). The hydrolysis would not occur in the presence of EZA (Fig. 3) possibly because the
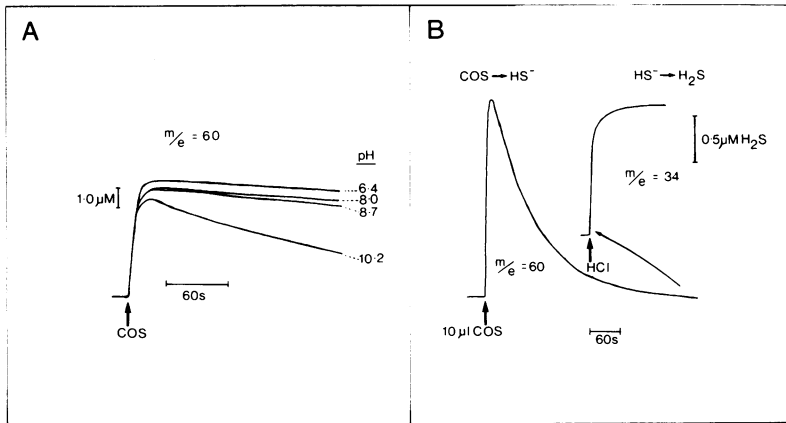
Figure 1. Effect of pH upon the rate of spontaneous hydrolysis of COS. A, Aliquots of an acidified (20 mM HCl) solution of COS were added to solutions of 25 mM BTP/HCl at various pH values at 30°C, in the closed MS cuvette. The signal at $m/e = 60$ was monitored. B, An aliquot of COS solution was added to 25 mM BTP/HCl at pH 10.6 and COS hydrolysis was monitored at $m/e = 60$. After complete hydrolysis, the HS^- was partially converted to H_2S by the addition of 2 N HCl to lower the pH to about 7. The term H_2S in the figure refers to the sum of H_2S and HS^-. The appearance of H_2S was monitored at $m/e = 34$ and the response was calibrated by the addition of aliquots of $Na_2S \cdot 9H_2O$ solution. From the data of (B) it can be calculated that the [COS] of the stock solution was 8.7 mM.
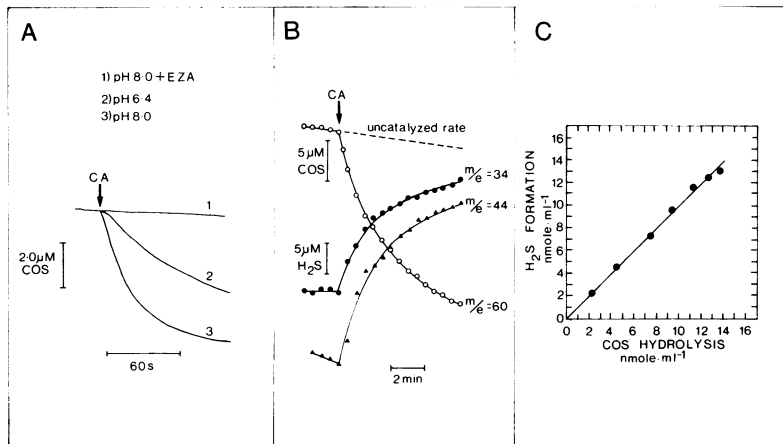
Figure 2. Catalysis of COS hydrolysis by CA. A, CA (104 WA units·mL^{-1}) was added to solutions of 6 μM COS in 25 mM BTP/HCl at pH 8.0 or 6.4. The [EZA] was 50 μM. The hydrolysis of COS was monitored at $m/e = 60$. B, CA (104 WA units·mL^{-1}) was added to a solution of 30 μM COS at pH 7.0 and the progress of COS hydrolysis (O), H_2S/HS^- formation (●), and CO_2 formation (Δ) were monitored at $m/e = 60, 34$, and 44, respectively. All three masses were monitored simultaneously using the mass peak jumping mode of the MS. No attempt was made to calibrate the $m/e = 44$ signal in this case since changes are due to both CO_2 production and CS^+. C, Stoichiometry of COS hydrolysis and $H_2S + HS^-$ production, derived from the data shown in (B). The term H_2S in both (B) and (C) refers to the sum of H_2S and HS^-.

intracellular CA would be inhibited. One cannot, however, totally rule out significant accumulation of COS in the cells because the volume of the reaction mixture occupied by the cells was very small (<0.2%).

Inhibition of COS Uptake by CO_2

The uptake of COS was drastically reduced by the presence of DIC (Figs. 3C and 5). The uptake from 2.7 μM COS was much more sensitive to inhibition than uptake from 27 μM COS (Fig. 5B). We have plotted the rate of COS uptake against the [CO$_2$] measured by MS in the extracellular medium just before COS addition (Fig. 5B). Since *Synechococcus* UTEX 625 rapidly and effectively removes CO_2 from the medium (4, 8, 19) upon illumination, one cannot merely assume that the [CO$_2$] upon the addition of COS is that calculated from the appropriate equilibrium coefficient for the HCO$_3^-$/CO$_2$ system. For each measurement of the COS uptake rate, the steady state [CO$_2$] was monitored at $m/e = 44$ (Fig. 5A). Then COS at 2.7 or 27 μM final concentration was added and the rate of COS uptake was measured (Fig. 5A). In the presence of 27 μM COS, and to a lesser extent with 2.7 μM COS, the [CO$_2$] would actually have risen from the initial, measured [CO$_2$] value upon the addition of COS (Fig. 6). This would have the effect of moving the data points in Figure 5B to the right. Obviously, determining the exact

nature of the interaction between CO_2 and COS uptake is difficult.

Inhibition of CO_2 Uptake by COS

When *Synechococcus* UTEX 625 cells were illuminated they rapidly took up CO_2 from the extracellular medium (Figs. 5A and 6) with the result that the HCO$_3^-$/CO$_2$ system was moved far from equilibrium. Upon the addition of COS (Fig. 6) a rapid increase in the extracellular [CO$_2$] was observed, followed by a slower rise to a [CO$_2$] close to the expected equilibrium value. Addition of CA at this point did not result in much further increase in the [CO$_2$] (Fig. 6). These experiments were carried out at low [Na$^+$] to prevent concomitant HCO$_3^-$ transport (15). We interpret the fast rise in the extracellular [CO$_2$] as being due to rapid leakage of the free CO_2 from the cells. The slower rise to the equilibrium [CO$_2$] was due to the reequilibration of the extracellular HCO$_3^-$/CO$_2$ system as a result of HCO$_3^-$ dehydration (19) in a system that could not now transport the CO_2. The effect of COS was rapid (Fig. 6) as expected for a compound directly causing inhibition of CO_2 transport.

We also examined the effect of COS upon CO_2 transport in several other ways. These studies were carried out in the absence and in the presence of concomitant HCO$_3^-$ transport. The results obtained in the absence of HCO$_3^-$ transport are discussed first. All cell samples used showed only very small
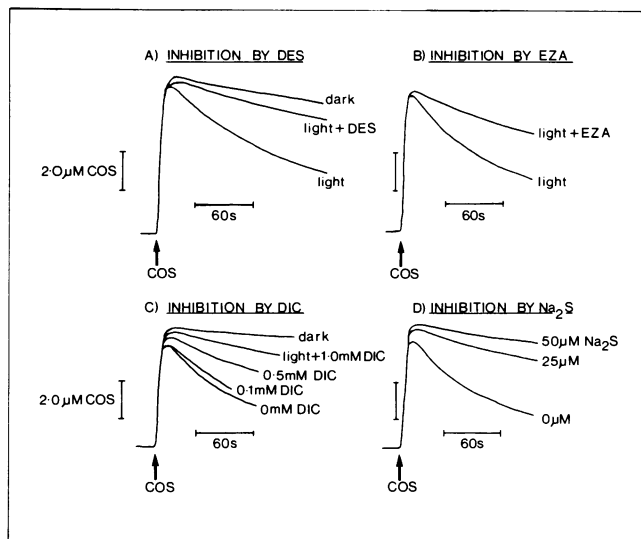
Figure 3. Catalysis of COS hydrolysis by *Synechococcus* UTEX 625. COS (7–8 μM) was added to cell suspensions (7.5–8.5 μg Chl·mL^{-1}) in 25 mM BTP/HCl (pH 8.0) and hydrolysis was monitored at m/e = 60. The [DES] was 10 μM (A), the [EZA] was 50 μM (B) with a preincubation period of 2 min with the inhibitor and the [Na$_2$S·9H$_2$O] was at 25 or 50 μM (D). Cells were at the CO$_2$ compensation point except in those cases where DIC (K$_2$CO$_3$) was added (C). The 2.0 μM COS scale bar is applicable to all four figures. The DES and EZA were added as ethanol solutions. The final ethanol concentration (0.1% v/v) had no effect upon COS uptake.

DIC accumulations in the absence of added 25 mM Na$^+$, as monitored by Chl a fluorescence yield (16, 20), thus demonstrating a lack of significant HCO$_3^-$ transport (data not shown). The effect of COS upon active CO$_2$ transport was measured in three ways. In one method (Fig. 7A), 25 μM K$_2$^{13}CO$_3$ was added to cells in the light either in the absence of COS or to cells to which 30 μM COS had been added 15 s previously (Fig. 7A). In the absence of COS, only a small rise in the [^{13}CO$_2$] of the medium occurred. Thus, a functioning CO$_2$ transport system removed the ^{13}CO$_2$ from the medium almost as fast as it was formed from dehydration of the H^{13}CO$_3^-$. In the presence of COS this did not occur and the [^{13}CO$_2$] of the medium rose to a value at or close to the equilibrium value (Fig. 7A). The amount of COS hydrolyzed in the 15 s before the addition of ^{13}C-bicarbonate was estimated in a separate run to be less than 10% and the [HS$^-$] thus produced would have been less than 3 μM. This [HS$^-$] would have had little effect upon CO$_2$ transport compared to the 30 μM COS (GS Espie, AG Miller, DT Canvin, unpublished results). The second measure of CO$_2$ transport involved pulsing the cell suspensions with an acidified CO$_2$ solution, which generates a [CO$_2$] in the cell suspension that is transiently greatly above the low [CO$_2$] that would exist at equilibrium (19). The rate of CO$_2$ transport by *Synechococcus* UTEX 625 is fast enough that a much more rapid depletion of CO$_2$ occurs in the presence of illuminated cells than due to the already rapid hydration of CO$_2$ to HCO$_3^-$ that occurs even in the absence of cells (Fig. 7B). The pulsing method gives only a semiquantitative measure of the rate of CO$_2$ transport because the apparent uptake of CO$_2$ is confounded by CO$_2$
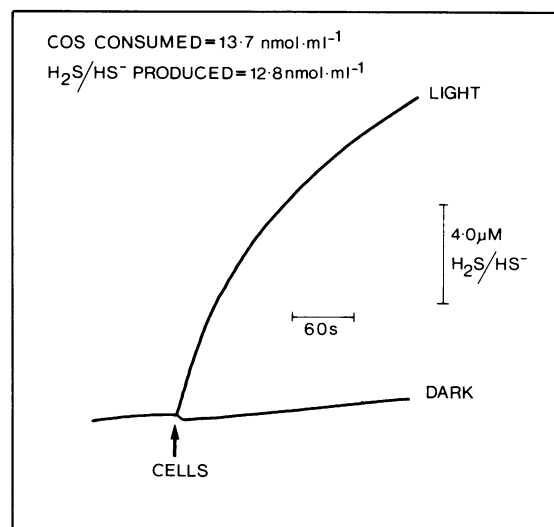

Figure 4. Formation of H$_2$S/HS$^-$ from COS by illuminated *Synechococcus* UTEX 625. A saturated solution of COS was added to 6 mL 25 mM BTP/HCl (+25 mM NaCl) at pH 6.95 to yield a final [COS] of 51.5 μM in the stoppered MS cuvette. The temperature was 30°C and the photon flux density was 800 μE·m^{-2}·s^{-1}. The magnitude of the m/e = 60 signal corresponding to the initial [COS] was recorded and then the MS was tuned so that H$_2$S formation (m/e = 34) could be continuously recorded. Washed cells (suspended in 200 μL buffer) were added to the cuvette to yield a final Chl concentration of 9.04 μg·mL^{-1}. After a period of COS hydrolysis and H$_2$S formation by the cells, the magnitude of the m/e = 60 signal was measured to determine the amount of COS remaining. Known concentrations of Na$_2$S·9H$_2$O were used to calibrate the m/e = 34 signal in terms of the total [H$_2$S + HS$^-$] at pH 6.95. A separate experiment was performed in the dark. In a second experiment, in which the cells in the light were allowed to consume 17.8 nmol·mL^{-1} COS there was a production of 17.2 nmol·mL^{-1} H$_2$S/HS$^-$. In a third experiment, the respective values were 11.1 nmol·mL^{-1} and 10.0 nmol·mL^{-1}.

hydration which occurs simultaneously. Transport of CO$_2$, however, as measured by this method, was severely inhibited by COS concentrations as low as 13 μM (Fig. 7B).

The third means of investigating the effect of COS upon CO$_2$ transport was to examine the rate of depletion of extracellular ^{13}CO$_2$ upon illumination of the cells (Fig. 7C). In the presence of 30 μM COS the rate of ^{13}CO$_2$ uptake was severely inhibited.

The effect of COS upon CO$_2$ transport was also investigated when HCO$_3^-$ transport was permitted by the addition of 25 mM Na$^+$ (Fig. 8). In this case, upon the addition of 25 μM K$_2$^{13}CO$_3$ in the presence of 30 μM COS, the [^{13}CO$_2$] in the medium rose not only to the equilibrium value as it did in the absence of HCO$_3^-$ transport (Fig. 7A) but far above it (Fig. 8A). This was dramatically evident upon the addition of CA to rapidly cause HCO$_3^-$/CO$_2$ equilibration (Fig. 8B). Since it was [^{13}CO$_2$] (m/e = 45) being monitored, the CO$_2$ appearing in the medium in the presence of COS must have resulted from the Na$^+$-dependent transport of H^{13}CO$_3^-$ followed by its intracellular dehydration to ^{13}CO$_2$. The same efflux of ^{13}CO$_2$ was not seen in the presence of 16 μM Na$_2$S or 25 μM ^{12}C-DIC (data not shown). Thus, the efflux of ^{13}CO$_2$ was caused by COS itself and not from its hydrolysis products, CO$_2$ and
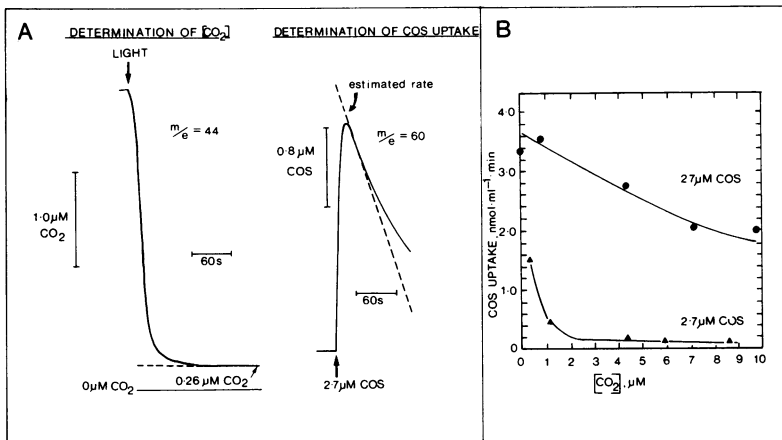
Figure 5. Inhibition of COS uptake by CO_2. A, Protocol used for determining the relevant extracellular [CO_2]. Cells (6.8–7.1 μg·Chl·mL^{-1}) were illuminated in the presence of various [DI^{12}C]. The steady state [CO_2] was monitored at m/e = 44. The MS was then set to monitor COS hydrolysis at m/e = 60. In the actual case presented, the [DIC] was 200 μM and the Chl concentration was 6.8 μg·mL^{-1}. B, COS hydrolysis at 2.7 or 27 μM at various extracellular [CO_2]. Incubations were in 25 mM BTP/HCl, pH 8.0 with 100 μM NaCl. Under these conditions very little HCO$_3^-$ transport occurred (data not shown), as monitored by Chl a fluorescence yield (16, 21).
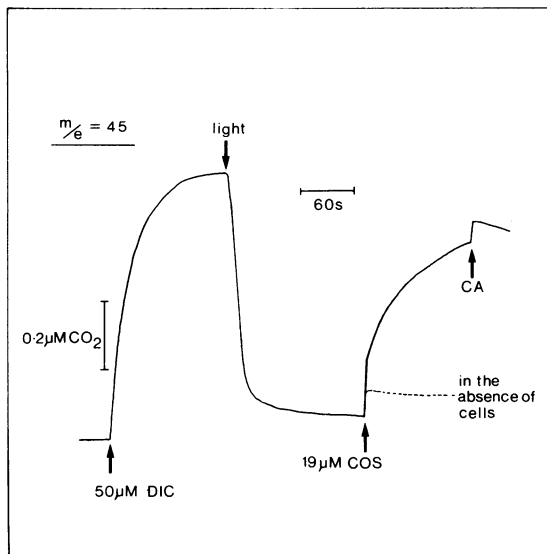

Figure 6. Effect of COS addition upon the extracellular [CO_2] in the absence of HCO$_3^-$ transport. Cells were incubated with 50 μM K$_2$^{13}CO$_3$ in 25 mM BTP/HCl (pH 8.0) and 100 μM NaCl. Chl concentration was 8.8 μg·mL^{-1}. The extracellular [^{13}CO$_2$] was monitored at m/e = 45. COS was added to a final concentration of 19 μM and CA at 52 WA units·mL^{-1}. The dashed line indicates the change in m/e = 45 signal seen upon COS addition in the absence of cells and is due to ^{13}CS$^+$ formed from ^{13}COS in the MS. Fluorescence measurements showed the lack of HCO$_3^-$ transport (16, 21) (data not shown).

HS$^-$. The maximum extent of COS hydrolysis that occurred before the addition of the ^{13}C-bicarbonate was measured separately as being no more than 10%. In the presence of iodoacetamide, to substantially reduce CO_2 fixation (23) and thus depletion of DI^{13}C from the system, ^{13}CO$_2$ efflux continued for an extended period (Fig. 8A). The ^{13}CO$_2$ efflux was near maximal at a concentration of 70 μM COS (data not shown).

In the absence of DIC transport, the Chl a fluorescence yield of *Synechococcus* UTEX 625 is close to the maximal value, F_M (16). When either CO_2 or HCO$_3^-$ transport is initiated, a drop in the fluorescence yield is observed, even in the absence of CO_2 fixation (16, 20). The majority (70–80%)

of the drop in fluorescence yield is due to q-quenching (21). This increase in q-quenching is correlated with an increased rate of O_2 photoreduction, both in the presence and absence of CO_2 fixation (21). How DIC transport causes this increase in O_2 photoreduction and q-quenching remains unknown, but there is a good correlation between the degree of quenching and the extent of DIC accumulation (20). The Chl a fluorescence yield thus serves as a valuable monitor of the extent of DIC transport and accumulation (16, 20). When 25 μM K$_2$^{13}CO$_3$ was added to cells in the absence of Na$^+$ only a small amount of quenching was observed and the extracellular [^{13}CO$_2$] remained low (data not shown). The small amount of quenching indicates only a small amount of DIC accumulation which, in the absence of HCO$_3^-$ transport due to the lack of Na$^+$ (7), is due to CO_2 transport resulting from the slow rate of HCO$_3^-$ dehydration at pH 8.0 (7). When K$_2$^{13}CO$_3$ was added in the presence of 25 mM Na$^+$ considerable quenching occurred (Fig. 9). This shows that the major accumulation of DIC, resulting in Chl a fluorescence quenching, in these cells was due to HCO$_3^-$ transport. The transport of CO_2 certainly did occur, as shown by the maintenance of the extracellular [^{13}CO$_2$] below the equilibrium value (Fig. 9), but the extent of DIC accumulation due to CO_2 transport, and the associated Chl a fluorescence quenching, would have been limited by the slow rate of CO_2 production from the extracellular HCO$_3^-$ (see Fig. 5A). When K$_2$^{13}CO$_3$ was added in the presence of 26 μM COS and 25 mM Na$^+$, the initial rate of Chl a fluorescence quenching was not affected but the maximum extent of quenching was reduced by 35% (Fig. 9). This suggests that COS had little effect upon the actual rate of HCO$_3^-$ transport but that the extent of DIC accumulation was reduced as a result of CO_2 leakage (Fig. 9). In the absence of COS, the leaked CO_2 would be returned to the cells by the CO_2 transport system (Fig. 9). Three minutes of N_2-bubbling were sufficient to remove more than 95% of the added COS (data not shown). Addition of K$_2$^{13}CO$_3$, after removal of the COS, yielded fluorescence quenching and extracellular [^{13}CO$_2$] similar to those obtained before COS addition (Fig. 9). An addition of 12 μM Na$_2$S at this point caused some increase in quenching and [^{13}CO$_2$] following K$_2$^{13}CO$_3$ addition, but much less than was obtained upon the addition of COS (Fig. 9). Less than 3 μM H$_2$S/HS$^-$ would have resulted
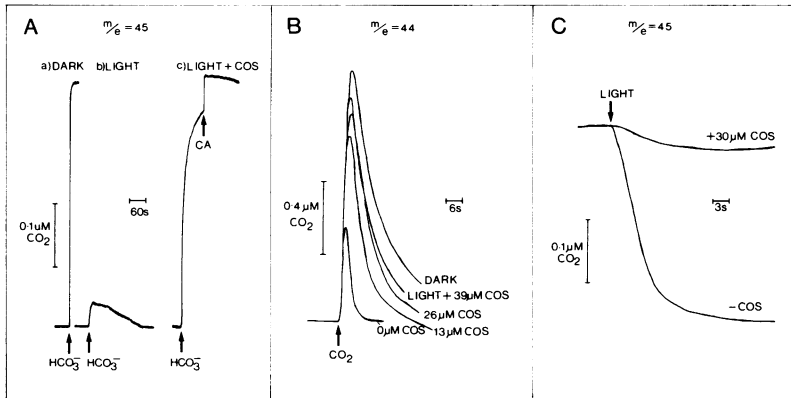
Figure 7. Inhibition of CO_2 transport by COS in the absence of HCO_3^- transport. Cells (7.1–7.5 μg Chl·mL^{-1}) were incubated in 25 mM BTP/HCl (pH 8.0) and 100 μM NaCl. The absence of HCO_3^- transport (data not shown) under these conditions was revealed by measurement of the Chl a fluorescence yield (16, 21). A, Separate cell suspensions were used for runs a, b, and c. (a) 25 μM K$_2^{13}$CO$_3$ added to cells in the dark. The extracellular [^{13}CO$_2$] was monitored at m/e = 45. (b) 25 μM K$_2^{13}$CO$_3$ added to cells in the light. (c) As for (b), but with 19 μM COS present. B, Cell suspensions were pulsed with CO_2 (final concentration 2.1 μM) in small aliquots of acidified water saturated at 0°C with 5% CO_2. The extracellular [^{12}CO$_2$] was monitored at m/e = 44. COS was present at 0, 13, 26, or 39 μM, as indicated. C, Cells were incubated with 25 μM K$_2^{13}$CO$_3$ in the absence or presence of 30 μM COS. Extracellular [^{13}CO$_2$] was monitored at m/e = 45.
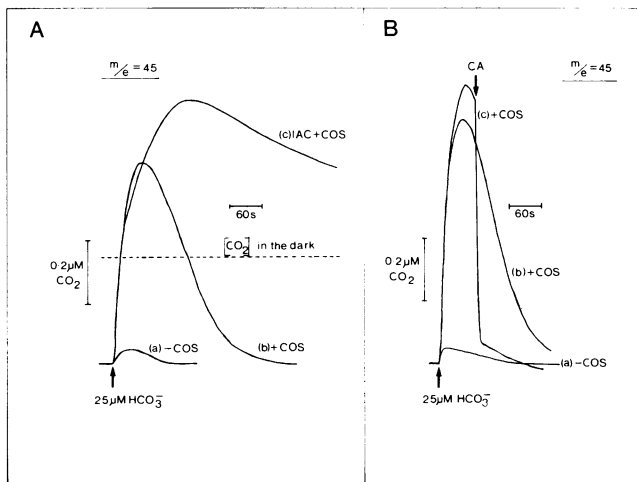
Figure 8. Inhibition of CO_2 transport by COS in the presence of HCO_3^- transport. Cells (7.6–7.9 μg Chl·mL^{-1}) were incubated in 25 mM BTP/HCl (pH 8.0) and 25 mM NaCl. The presence of HCO_3^- transport (data not shown) under these conditions was revealed by measurement of the Chl a fluorescence yield (16, 21). A, 25 μM K$_2^{13}$CO$_3$ was added to cells in the light in the absence of COS (curve a), in the presence of 30 μM COS (curve b), and in the presence of 30 μM COS and 3.3 mM iodoacetamide (curve c). Cells were preincubated with the iodoacetamide in the light at the CO_2 compensation point for 5 min before the addition of the K$_2^{13}$CO$_3$. The extracellular [^{13}CO$_2$] was monitored at m/e = 45. The dashed line represents the [^{13}CO$_2$] observed upon addition of 25 μM K$_2^{13}$CO$_3$ to cells in the dark. B, As for (A) but iodoacetamide was not present in (c) and CA (52 WA units·mL^{-1}) was added at the time indicated.

from COS hydrolysis before the addition of K$_2^{13}$CO$_3$ (Fig. 9, curve 2).

The results obtained by monitoring the quenching of Chl a fluorescence (Fig. 9) strongly suggested that COS did not inhibit HCO_3^- transport. The ultimate quenching seen in the presence of COS was lower (Fig. 9), probably due to the inability of the cells to form a normal sized internal pool of DIC because of the significant CO_2 leakage that occurs when the CO_2 pump is inhibited (Fig. 8). More direct tests of a possible effect of COS upon HCO_3^- transport substantiated this belief (Figs. 10 and 11).
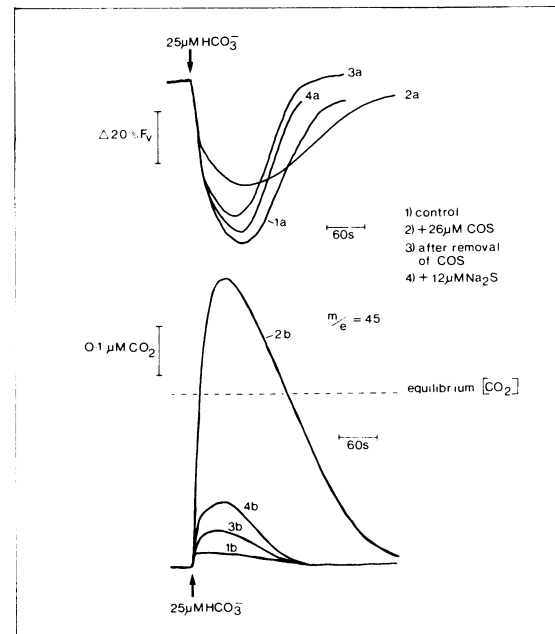
Figure 9. Quenching of Chl a fluorescence as a consequence of HCO_3^- transport when CO_2 transport is inhibited by COS. The cells were allowed to reach the CO_2-compensation point in the presence of 25 mM NaCl. Then 25 μM K$_2^{13}$CO$_3$ was added and the effects upon Chl a fluorescence yield and the extracellular [^{13}CO$_2$] were monitored. Conditions were as follows: No COS present (1a, b curves); 26 μM COS present (2a, b curves); after removal of the 26 μM COS by N$_2$-bubbling (3a, b curves) and after the subsequent addition of 12 μM Na$_2$S (4a, b curves). The experiments were carried out in succession on the same cell suspension. The Chl concentration was 7.6 μg·mL^{-1}. The upper set of curves describe the changes in Chl a fluorescence yield and the lower set of curves represent the changes in the extracellular [CO_2].

In fairly dense cell suspensions at pH 8.0, the rate of photosynthesis in the presence of 25 μM DIC is limited by the rate of HCO_3^- transport (16). Under these conditions (Fig. 10A), the presence of 70 μM COS had little effect upon the initial rate of CO_2 fixation as monitored by ^{14}C incorporation into acid-stable products. The steady state rate of photosyn-
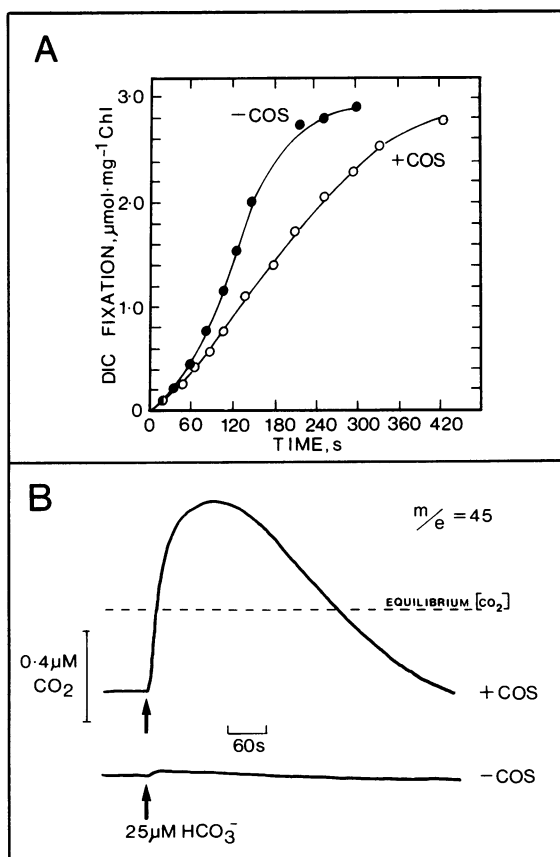
Figure 10. Effect of COS upon CO_2 fixation. Cells were incubated in 25 mM BTP/HCl (+25 mM NaCl) at pH 8.0 and allowed to reach the CO_2 compensation point. The cells were then further incubated for 60 s in the absence (●) or presence (O) of 74 μM COS. The Chl concentrations were 8.73 and 9.50 μg·mL^{-1}, respectively. The cells were illuminated (500 μE·m^{-2}·s^{-1}). A solution containing both H^{13}CO$_3^-$ and H^{14}CO$_3^-$ (2.99 μCi·μmol^{-1} carbon) was added to yield a final [HCO$_3^-$] of 25 μM. Samples of 50 μL were withdrawn at intervals and injected into 1 mL methanol. The samples were later analyzed for acid stable ^{14}C activity (A). The [^{13}CO$_2$] in the medium was continuously recorded (B) by MS (m/e = 45) while the samples for ^{14}C analysis were being taken. The concentrations of ^{12}CO$_2$ (m/e = 44) and ^{14}CO$_2$ (m/e = 46) were below detection limits. The equilibrium [^{13}CO$_2$] corresponds to the [^{13}CO$_2$] in the medium when 25 μM H^{13}CO$_3^-$ was added to the cells in the dark. Similar results to those of (A) and (B) were obtained in two other experiments.

thesis was substantially reduced, presumably because of the leakage of CO_2 from the cells (Fig. 10B) due to the COS inhibition of the CO_2 pump. The $K_{1/2}$ for HCO$_3^-$ transport is considerably higher than the $K_{1/2}$ for CO_2 transport (GS Espie, AG Miller, DT Canvin, unpublished results). It is to be expected that as the extracellular [DIC] falls due to CO_2 fixation (Fig. 10A) that the $K_{1/2}$ for whole cell photosynthesis will rise if the high affinity CO_2 pump is inhibited. The use of the silicone fluid centrifugation technique showed that 100 μM COS had little or no effect upon the initial rate of DIC transport (Fig. 11). The transport was initiated by the addition of HCO$_3^-$ and under these conditions almost all the DIC transport can be attributed to HCO$_3^-$ transport (16).

Concentrations of CS_2 and N_2O as high as 100 μM had no
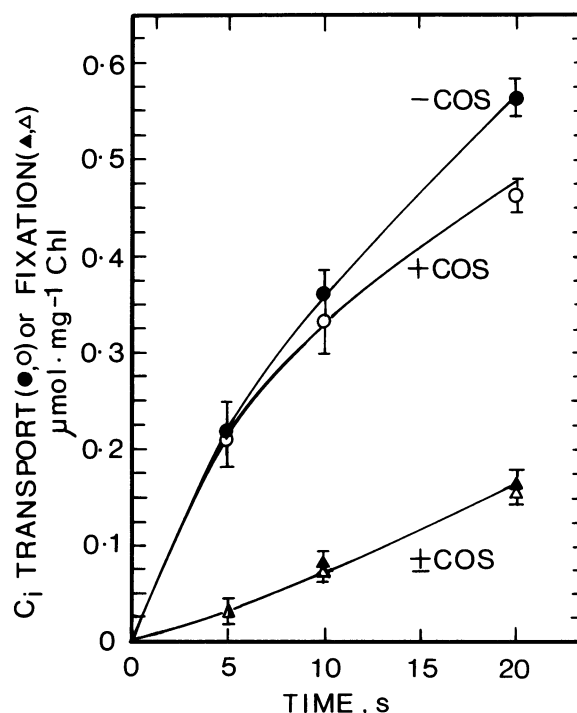
Figure 11. Effect of COS upon HCO$_3^-$ transport. Cells were incubated in 25 mM BTP/HCl (+25 mM NaCl) at pH 8.0 in an O$_2$-electrode cuvette. The cells were allowed to reach the CO_2 compensation point. Samples (100 μL) of the cell suspension were then layered over 100 μL silicon fluid in N$_2$-purged 400 μL microfuge tubes. Below the silicon fluid layer was 100 μL 2 N KOH in 10% methanol. Individual tubes were then placed in an illuminated (300 μE·m^{-2}·s^{-1}) microfuge. To the tubes were then added 10 μL of water (●) or 10 μL COS saturated water (O). The final [COS] was 100 μM. After 15 s, 10 μL of H^{14}CO$_3^-$ (6.0 μCi·μmol^{-1} carbon) was added. The transport and fixation of ^{14}C was stopped at various times by turning on the microfuge. The samples were analyzed for total ^{14}C (●, O) and acid stable (▲, △) activity in the terminating solution (18). The means ± SE (n = 4) are given. The intracellular [DIC] attained after 20 s in the absence of COS was 7.5 mM and in the presence of 100 μM COS was 6.2 mM, assuming 75 μL cell water·mg^{-1} Chl.

effect upon CO_2 transport as measured by any of the three methods described in Figure 7 (data not shown). The pattern of fluorescence quenching and recovery after the addition of HCO$_3^-$ was also unaffected (data not shown), indicating a lack of inhibition of either HCO$_3^-$ transport or CO_2 fixation by these gases.

DISCUSSION

COS is a structural analog of CO_2 with essentially the same electronic configuration (10). Both COS and CO_2 are linear molecules although COS, being asymmetric, has a dipole moment (10). Like CO_2, COS is susceptible to OH$^-$ catalysed hydration at high pH (Fig. 1) or at lower pH in the presence of CA (Fig. 2). Unlike CO_2, the hydration of COS does not result in the formation of a stable intermediate, as neither monothiocarbonic acid nor monothiocarbonate ion are stable at room temperature (25, 29). COS is an alternate substrate for Rubisco and the products of the reaction of COS with

ribulose-1,5-bisphosphate are 3-phosphoglycerate and 3-phospho-1-thioglycerate (13). Interestingly, in terms of possible mechanisms for CO_2 and COS transport, COS forms thiocarbamates with uncharged amines (9). The ratios of the rate constants for the addition to amines for CO_2:COS:CS_2 are in the order of 10^5:10^3:1, respectively (9). Thus, COS reacts at a reasonable rate with amines compared to CO_2, whereas CS_2 does not. Some steric differences might be expected during the interaction of CO_2 and COS with a CO_2 transport system, due to the larger size of the S atom. The Van der Vaals radius of the S atom is about 36% larger than that of the O atom (14). The C=S bond of COS is 1.56 Å long compared to 1.6 Å for the C=O bond (10). The C=O bond has essentially the same length as in the CO_2 molecule (10). Thus, the COS molecule will be about 17% longer than the CO_2 molecule due to the greater length of the C=S bond.

COS inhibited active CO_2 transport by *Synechococcus* UTEX 625 much more effectively than it inhibited HCO_3^- transport. When 25 mM Na^+ was present to allow rapid HCO_3^- transport, the addition of $K_2^{13}CO_3$ in the presence of COS caused the extracellular [$^{13}CO_2$] to rise dramatically above the equilibrium value (Fig. 8). This rise in the extracellular [$^{13}CO_2$] in the presence of COS can only be interpreted as due to active transport of $H^{13}CO_3^-$ followed by its intracellular dehydration to $^{13}CO_2$ which then leaked from the cells down its concentration gradient (Fig. 8). In the absence of COS, the active CO_2 transport system scavenged the leaked $^{13}CO_2$ as fast as it leaked from the cells (Fig. 8). The initial rate of quenching of Chl a fluorescence upon the addition of $K_2^{13}CO_3$ was very similar in the absence and presence of COS (Fig. 9). During the initial period of fluorescence quenching, there was a net leakage of CO_2 from the cells (Fig. 9). Thus the fluorescence quenching could only have been the result of net HCO_3^- influx which proceeded at a rapid rate in the presence of COS.
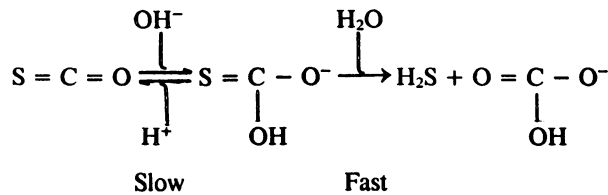
The lack of COS inhibition of HCO_3^- transport was confirmed by using the silicone fluid centrifugation method (Fig. 11). The steady-state rate of CO_2 fixation, but not the initial rate, was significantly reduced in the presence of 75 μM COS (Fig. 10). Such a reduction in the rate of CO_2 fixation is not unexpected when one considers that a considerable amount of the HCO_3^- is converted to CO_2 which then leaks from the cells (Figs. 8 and 10). Ogawa and Togasaki (24) recently reported that both CO_2 and HCO_3^- transport were inhibited and that CO_2 fixation by *Synechococcus* PCC 7942 was completely and irreversibly inhibited by COS. It is unclear why their results differ so markedly from ours (Figs. 10 and 11). Ogawa and Togasaki (24) attributed the inhibition of CO_2 fixation to displacement of the activator CO_2 on Rubisco by COS (13). However, our results (Fig. 4) indicate that most of the COS taken up by the cells was converted to H_2S. The COS-dependent O_2 evolution observed under these conditions (data not shown) indicates not only that COS breakdown results in CO_2 formation, as well as H_2S, but that the CO_2 produced can be fixed by an active Rubisco. Ogawa and Togasaki (24) used considerably higher COS concentrations and pH 7.0 instead of pH 8.0. If COS was converted to H_2S by their organism the effects they observed may be due in part to H_2S/HS^- as well as COS.

Although the extracellular [$^{13}CO_2$] was forced far above its equilibrium level in the presence of COS (Fig. 8), it must be remembered that the intracellular [CO_2] that results from active HCO_3^- transport can be more than 10,000-fold higher than the extracellular [CO_2] (19). Using $H^{13}C^{18}O_3^-$ we have found that most of the CO_2 that leaks from the cells in the presence of COS is $^{13}C^{16}O_2$, demonstrating that the intracellular HCO_3^-/CO_2 dehydration-hydration cycle is rapidly catalyzed (AG Miller, DT Canvin, unpublished data). It seems that if cells are to most rapidly perform CO_2 fixation at low [DIC] then active CO_2 transport as well as active HCO_3^- transport is necessary. The return of leaked CO_2 to the cells via the active CO_2 transport system will certainly require a further input of energy. In nature, various balances between the CO_2 and HCO_3^- transport activities will probably exist depending upon whether DIC or energy is in shortest supply. It is worth noting that *Synechococcus* seems to rely mainly on CO_2 transporting ability when grown at high [DIC] (4, 17). The marine species of *Synechococcus* studied by Badger and Andrews (2, 3) showed a CO_2 efflux pattern during active HCO_3^- transport very similar to that seen with UTEX 625 (Fig. 8) in the presence of COS. Apparently, a different balance exists between the rates of CO_2 and HCO_3^- transport in this species. Factors such as the rate of intracellular HCO_3^- dehydration and the passive permeability of the cells to CO_2 may further influence the rate of CO_2 leakage during active HCO_3^- transport.

It was not possible to obtain detailed kinetic information about the effect of COS on CO_2 transport. The difficulty arose because CO_2 transport was so rapid it shifted the HCO_3^-/CO_2 system far out of equilibrium (Figs. 5 and 6) and because COS itself was taken up and metabolized (Fig. 4). It was not possible, therefore, to know exactly the [CO_2] and [COS] at any given time. The uptake of COS was inhibited by increasing [DIC] in an essentially competitive fashion (Figs. 3 and 5). We presume that CO_2 was the active species, not HCO_3^-, in the inhibition but these data do not conclusively show this. COS inhibited CO_2 transport (Fig. 7) as measured by CO_2 pulsing, CO_2 efflux in the presence of Na^+-dependent HCO_3^- transport (Fig. 8) and by the disequilibration of the HCO_3^-/CO_2 system upon illumination (Fig. 7). These experiments conclusively show that it was CO_2 transport, and not HCO_3^- transport, that was being inhibited by the presence of COS. Removal of COS, by bubbling the cell suspensions with N_2, resulted in a substantial recovery of CO_2 transport (Fig. 9). Taken together the results argue for a quite selective inhibition of the CO_2 transport system by COS.

Illuminated cells catalyzed the hydrolysis of COS to H_2S (Fig. 4), and presumably CO_2, by a process sensitive to the CA inhibitor EZA (Fig. 3B). Carbonic anhydrase itself catalyzed the stoichiometric hydrolysis of COS to H_2S (Fig. 2). There is only one previous report, of which we are aware, that demonstrates catalysis of COS hydrolysis by CA (5). These authors found that bovine erythrocyte CA catalyzed the breakdown of $CO^{35}S$ to $H_2^{35}S$ and ^{14}COS to $^{14}CO_2$ (5). The process was inhibited by acetazolamide. Our MS determination of COS hydrolysis has the advantage that a continuous record of the reaction progress was obtained (Fig. 2B). The rate of H_2S formation equaled the rate of COS breakdown at all

times (Fig. 2C), giving no evidence for the accumulation of significant amounts of the monothiocarbonate ion intermediate:

$$S = C = O \underset{H^+}{\overset{OH^-}{\rightleftharpoons}} S = C - O^- \overset{H_2O}{\longrightarrow} H_2S + O = C - O^-$$
$$\qquad\qquad OH \qquad\qquad\qquad\qquad OH$$

Slow   Fast

The rate of spontaneous breakdown of the monothiocarbonate ion has been reported to be rapid at low ionic strength at room temperature (25, 29). The addition of acid did not cause a reappearance of the $m/e = 60$ signal due to COS, either when COS was in the presence of bovine erythrocyte CA (Fig. 2) or cells (Fig. 3). This further shows that in neither case was there a substantial accumulation of the monothiocarbonate ion. Illuminated cells caused an irreversible disappearance of COS (Fig. 3) suggesting that almost all the COS taken up was converted to CO_2 and H_2S (Fig. 4). We presume that the COS was hydrolyzed by the same intracellular CA activity that catalyzes the efficient intracellular dehydration-hydration of the HCO_3^-/CO_2 system in cyanobacteria (3, 28, 30). This process is sensitive to EZA (28). The enhanced hydrolysis in the light may be due to an enhanced accumulation of COS within the cells mediated by the active CO_2 transport system. Although we found no evidence of intracellular accumulation of COS, we had to rely upon observing an increase in the extracellular [COS] that would occur upon cessation of COS transport and leakage of the accumulated COS back into the medium. The cell volume was less than 0.2% that of the medium, so that a 10-fold COS accumulation within the cells would result in only a 2% increase in the extracellular [COS] upon leakage back into the medium, even assuming no further COS hydrolysis within the cells. The light enhanced rate of COS hydrolysis was only about 10-fold and could be accounted for by only an increased 10-fold [COS] around the intracellular catalyst.

The disappearance of COS from the medium was inhibited by low concentrations of CO_2 (Figs. 3 and 5). Given the K_m (CO_2) value for CA-catalyzed hydration of CO_2 on the order of 20 mM CO_2 (26), one would not expect these low [CO_2] (Fig. 5) to so effectively reduce the rate of COS hydrolysis—even with considerable intracellular CO_2 accumulation (19). The effective inhibition of COS disappearance by CO_2 is more readily explained by assuming that CO_2 competed with COS for transport into the cells by the high affinity CO_2 transport system. By both MS and fluorescence studies we have determined that the $K_{1/2}$ (CO_2) for active CO_2 transport by air-grown cells at pH 8.0 is 0.2 to 0.4 μM CO_2 (GS Espie, AG Miller, DT Canvin, unpublished data).

A model proposed by Volokita et al. (31) would explain the light stimulation of COS hydrolysis. These authors have proposed that CO_2 transport by cyanobacteria involves an obligatory hydration of the CO_2 to HCO_3^- by an intrinsic CA-like moiety in the cell membrane (31). The CO_2 transporter, in effect, would act as a unidirectional, light stimulated CA (31). This intriguing model was put forward when it was thought that cyanobacteria lacked intracellular CA activity

(31). It is now evident that the HCO_3^-/CO_2 dehydration-hydration cycle is rapidly catalyzed within cyanobacterial cells (3, 28, 30) (AG Miller, DT Canvin, unpublished data). The initial arguments put forward for an obligatory hydration of CO_2 to HCO_3^- during its transport across the cell membrane have subsequently lost some of their appeal. It may be difficult, using intact cells, to determine whether CO_2 hydration occurs during transport or very soon after its entry into the cytoplasm as CO_2 itself.

How CO_2 interacts with the transport system is completely unknown. The lack of inhibition of CO_2 transport by either carbon disulfide, CS_2, or nitrous oxide, N_2O, even when present in concentrations greatly in excess of the CO_2 concentration (data not shown) suggests that hydrophobic bonding may not be important. The order of decreasing hydrophobicity is $N_2O > CS_2 > COS > CO_2$ (6, 10). Both N_2O and CS_2 are linear molecules and are isoelectronic with respect to CO_2 (14). The structure of N_2O is explained in terms of the resonance forms $N \equiv N^+ - O^-$ and $^-N = N^+ = O$ (14). Neither CS_2 nor N_2O are as susceptible to nucleophilic attack as CO_2 and COS (14). Infrared spectroscopy has demonstrated that N_2O displaced CO_2 from a hydrophobic site on CA (26). This site was originally thought to be the active site but may not have been since N_2O had little effect upon the rate of CO_2 hydration (26). Infrared spectroscopy has also demonstrated that N_2O binds to hydrophobic sites on both bovine serum albumin and Cyt C oxidase (6). Such studies indicate that if a hydrophobic bonding site for CO_2 was obligatory for transport, then inhibition by N_2O, and probably CS_2, would be likely. The observation that only COS inhibited CO_2 transport may be a reflection of a covalent bonding reaction obligatory for transport. A possibility for such a reaction would be that of carbamate formation with amine N (9).

LITERATURE CITED

1. **Andrews TJ, Abel KM** (1981) Kinetics and subunit interactions of ribulose bisphosphate carboxylase-oxygenase from the cyanobacterium Synechococcus sp. J Biol Chem **256**: 8445–8451
2. **Badger MR, Andrews TJ** (1982) Photosynthesis and inorganic carbon usage by the marine cyanobacterium Synechococcus sp. Plant Physiol **70**: 517–523
3. **Badger MR, Bassett M, Comins HN** (1985) A model for HCO_3^- accumulation and photosynthesis in the cyanobacterium Synechococcus sp. Plant Physiol **77**: 465–471
4. **Badger MR, Gallagher A** (1987) Adaptation of photosynthetic CO_2 and HCO_3^- accumulation by the cyanobacterium Synechococcus PCC 6301 to growth at different inorganic carbon concentrations. Aust J Plant Physiol **14**: 189–201
5. **Chengelis CP, Neal RA** (1979) Hepatic carbonyl sulfide metabolism. Biochem Biophys Res Commun **90**: 993–999
6. **Einarsdottir O, Caughey WS** (1988) Interactions of the anesthetic nitrous oxide with bovine heart cytochrome c oxidase. J Biol Chem **263**: 9199–9205
7. **Espie GS, Canvin DT** (1987) Evidence for Na^+-independent HCO_3^- uptake by the cyanobacterium Synechococcus leopoliensis. Plant Physiol **84**: 125–130

8. Espie GS, Miller AG, Birch DG, Canvin DT (1988) Simultaneous transport of CO₂ and HCO₃⁻ by the cyanobacterium *Synechococcus* UTEX 625. Plant Physiol **87**: 551–554

9. Ewing SP, Lockshon D, Jencks WP (1980) Mechanism of cleavage of carbamate anions. J Am Chem Soc **102**: 3072–3084

10. Ferm RJ (1957) The chemistry of carbonyl sulfide. Chem Rev **57**: 621–640

11. Goldhaber MB, Kaplan LR (1975) Apparent dissociation constants of hydrogen sulfide in chloride solutions. Mar Chem **3**: 83–104

12. Kaplan A, Badger MR, Berry JA (1980) Photosynthesis and the intracellular inorganic carbon pool in the blue-green alga *Anabaena variabilis*: Response to external CO₂ concentration. Planta **149**: 219–226

13. Lorimer GH, Pierce J (1989) Carbonyl sulfide: An alternative substrate for but not an activator of ribulose-1,5-bisphosphate carboxylase. J Biol Chem **264**: 2764–2772

14. Mackay KM, Mackay RA (1969) Introduction to Modern Inorganic Chemistry. International Textbook Co., Ltd., London

15. Miller AG, Canvin DT (1985) Distinction between HCO₃⁻ and CO₂-dependent photosynthesis in the cyanobacterium *Synechococcus leopoliensis* based on the selective response of HCO₃⁻ transport to Na⁺. FEBS Lett **187**: 29–32

16. Miller AG, Canvin DT (1987) The quenching of chlorophyll *a* fluorescence as a consequence of the transport of inorganic carbon by the cyanobacterium *Synechococcus* UTEX 625. Biochim Biophys Acta **894**: 407–413

17. Miller AG, Canvin DT (1987) Na⁺-stimulation of photosynthesis in the cyanobacterium *Synechococcus* UTEX 625 grown on high levels of inorganic carbon. Plant Physiol **84**: 118–124

18. Miller AG, Colman B (1980) Active transport and accumulation of bicarbonate by a unicellular cyanobacterium. J Bacteriol **143**: 1253–1259

19. Miller AG, Espie GS, Canvin DT (1988) Active transport of CO₂ by the cyanobacterium *Synechococcus* UTEX 625: measurement by mass spectrometry. Plant Physiol **86**: 677–683

20. Miller AG, Espie GS, Canvin DT (1988) Chlorophyll *a* fluorescence yield as a monitor of both active CO₂ and HCO₃⁻ transport by the cyanobacterium *Synechococcus* UTEX 625. Plant Physiol **86**: 655–658

21. Miller AG, Espie GS, Canvin DT (1988) Active transport of inorganic carbon increases the rate of O₂ photoreduction by the cyanobacterium *Synechococcus* UTEX 625. Plant Physiol **88**: 6–9

22. Miller AG, Turpin DH, Canvin DT (1984) Growth and photosynthesis of the cyanobacterium *Synechococcus leopoliensis* in HCO₃⁻-limited chemostats. Plant Physiol **75**: 1064–1070

23. Ogawa T, Omata T, Miyano A, Inoue Y (1985) Photosynthetic reactions involved in the CO₂-concentrating mechanism in the cyanobacterium, *Anacystis nidulans*. *In* WJ Lucas, JA Berry, eds, Inorganic Carbon Uptake by Aquatic Photosynthetic Organisms. American Society of Plant Physiologists, Rockville, MD, pp 287–304

24. Ogawa T, Togasaki RK (1988) Carbonyl sulfide: An inhibitor of inorganic carbon transport in cyanobacteria. Plant Physiol **88**: 800–804

25. Philipp B, Dautzenberg H (1965) Kinetische Untersuchungen zur Bildung und Zersetzung von Monothiocarbonat in wässriger Lösung. Z Physik Chem **229**: 210–224

26. Pocker Y, Sarkanen S (1978) Carbonic anhydrase: structure, catalytic versatility, and inhibition. Adv Enzymol **47**: 149–274

27. Shelp BJ, Canvin DT (1984) Evidence for bicarbonate transport and accumulation by *Anacystis nidulans*. Can J Bot **62**: 1398–1403

28. Spiller H, Wynns GC, Tu C (1988) Role of photosynthetic reactions in the activity of carbonic anhydrase in *Synechococcus* sp. (UTEX 2380) in the light. Inhibitor studies using the ¹⁸O-exchange in ¹³C/¹⁸O-labeled bicarbonate. Plant Physiol **86**: 1185–1192

29. Thompson HW, Kearton CF, Lamb SA (1935) The kinetics of the reaction between carbonyl sulphide and water. J Chem Soc **1935**: 1033–1037

30. Tu CK, Spiller H, Wynns GC, Silverman DN (1987) Carbonic anhydrase and the uptake of inorganic carbon by *Synechococcus* sp. (UTEX 2380). Plant Physiol **85**: 72–77

31. Volokita M, Zenvirth D, Kaplan A, Reinhold L (1984) Nature of the inorganic carbon species actively taken up by the cyanobacterium *Anabaena variabilis*. Plant Physiol **76**: 599–602